Translational Oncology 14 (2021) 101129

Contents lists available at ScienceDirect

Translational Oncology

journal homepage: www.elsevier.com/locate/tranon

Original Research

Luteolin promotes macrophage-mediated phagocytosis by inhibiting CD47 pyroglutamation

Zhiqiang Li[a,1], Xuemei Gu[b,1], Danni Rao[c,d,1], Meiling Lu[e], Jing Wen[a], Xinyan Chen[f], Hongbing Wang[f], Xianghuan Cui[a], Wenwen Tang[a], Shilin Xu[c,d], Ping Wang[b,a,*], Lei Yu[a,*], Xin Ge[g,*]

[a] Tongji University Cancer Center, Shanghai Tenth People's Hospital, School of Medicine, Tongji University, Shanghai 200092, China
[b] Shanghai Clinical Medical College, Anhui Medical University, Hefei 230031, China
[c] Department of Medicinal Chemistry, Shanghai Institute of Materia Medica, Chinese Academy of Sciences, Shanghai 201203, China
[d] University of Chinese Academy of Science, 19 Yuquan Road, Beijing 110039, China
[e] Department of Central Laboratory, Shanghai Tenth People's Hospital of Tongji University, School of Medicine, Tongji University, Shanghai 200092, China
[f] Putuo District People's Hospital, School of Life Sciences and Technology, Tongji University, Shanghai 200092, China
[g] Department of Clinical Laboratory Medicine, Shanghai Tenth People's Hospital, School of Medicine, Tongji University, Shanghai 200092, China

ARTICLE INFO

Keyword:
Luteolin
CD47-SIRPα
isoQC
Phagocytosis
Tumor immunotherapy

ABSTRACT

'Don't eat me' signal of CD47 is activated via its interaction with SIRPα protein on myeloid cells, especially phagocytic cells, and prevents malignant cells from anti-tumor immunity in which pyroglutamate modification of CD47 by glutaminyl-peptide cyclotransferase-like protein (isoQC) takes an important part evidenced by our previous report that isoQC is an essential regulator for CD47-SIRPα axis with a strong inhibition on macrophage-mediated phagoctyosis. Therefore, we screened for potential isoQC inhibitors by fluorescence-activated cell sorting assay and identified luteolin as a potent compound that blocked the pyroglutamation of CD47 by isoQC. We further demonstrated that luteolin directly bound to isoQC using pull-down assay and isothermal calorimetric (ITC) assay. In consistency, we showed that luteolin markedly abrogated the cell-surface interaction between CD47 and SIRPα in multiple myeloma H929 cells and consequently promoted the macrophage-mediated phagocytosis. Collectively, our study discovered a promising lead compound targeting isoQC, luteolin, which functions distinctly from current CD47 antibody-based drugs and therefore may potentially overcome the clinical side effects associated with CD47 antibody treatment-induced anemia.

Introduction

Cancer immunotherapy has been broadly employed as a therapeutic strategy against cancer over the past decade [1]. Cancer cells can escape from immune surveillance by hijacking the inhibitory checkpoint pathways [2–4]. CD47 is a highly expressed inhibitory ligand on many types of tumor cells and can directly interact with the receptor signal regulatory protein alpha (SIRPα) that abundantly expresses on phagocytic cells, which serves as the major 'don't eat me' signal to stop the elimination of tumor cells by macrophage-mediated phagocytosis and finally facilitates immune evasion of tumors [4]. In this context, CD47-SIRPα axis plays an essential role in regulation of anti-tumor immunity, backed up by relevant studies demonstrating that antibodies targeting the CD47-SIRPα interaction can effectively terminate various types of cancer in mice and humans [5,6]. However, endogenous CD47 is also expressed on normal cells (i.e. erythrocytes), leading to undesirable side effects associated with anemia when cancer patients were treated with CD47 monoclonal antibodies during clinical trials [7]. In addition, antibody-

Abbreviations: BMDM, Bone marrow derived macrophage; BSA, Bovine Serum Albumin; CD47, Cluster of Differentiation 47; DEPC, Diethyl pyrocarbonate; DTT, Dithiothreitol; DMEM, Dulbecco's Modified Eagle Medium; DMSO, Dimethyl sulfoxide; EDTA, Ethylene Diamine Tetraacetic Acid; FACS, Fluorescence- activated cell sorting; FBS, Fetal bovine serum; GEO, Gene Expression Omnibus; GST, Glutathione s-transferase; ITC, Isothermal Titration Calorimetry; M-CSF, Macrophage-Colony Stimulating Factor; SDS-PAGE, Sodium Dodecyl Sulfate Polyacrylamide Gel Electrophoresis; PBS, Phosphate-buffered saline; PCR, Polymerase Chain Reaction; PMSF, Phenylmethanesulfonylfluoride; pGlu, Pyroglutamate; QC, Glutaminyl cyclases; isoQC, Glutaminyl-peptide cyclotransferase-like protein; SIRPα, Signal regulatory protein alpha.

* Corresponding authors.
E-mail addresses: wangp@tongji.edu.cn (P. Wang), yulei31@tongji.edu.cn (L. Yu), xin.ge@tongji.edu.cn (X. Ge).
[1] These authors have contributed equally to this work and share first authorship.

https://doi.org/10.1016/j.tranon.2021.101129
Received 10 March 2021; Received in revised form 5 May 2021; Accepted 17 May 2021

based drugs are economically unsustainable for clinical translation due to the high costs resulted from limited production rates, strict preservation requirements and stringent demands on transportation. Hence, there is a clear need for identifying alternative agents to disrupt CD47-SIRPα interaction.

Glutaminyl-peptide cyclotransferase-like protein (isoQC) is exclusively resident in the Golgi apparatus, which is absent from mature red blood cells along with other cell organelles (i.e. nucleus, mitochondria, endoplasmic reticulum etc.) [8,9] and catalyzes the formation of N-terminal pyroglutamate (pGlu) by converting glutamate/glutamine to pGlu residue similar as the secretory isoenzyme Glutaminyl cyclases (QC) [1,10,11]. Prior researches have indicated that isoQC is the critical regulator of pGlu modification of CD47 N-terminal peptide and resultantly affects the interaction between CD47 and SIRPα [12,13]. Interference with isoQC activity enhances antibody-dependent cellular phagocytosis and leads to a major increase in neutrophil-mediated killing of tumor cells in vivo [12], suggesting a promising role of isoQC as the therapeutic target of anti-tumor immunity.

In the past decades, bioactive natural compounds have been reported to work as therapeutic agents for treating various human disorders such as cancers [14], inflammation [15], cardiovascular [16] and neurodegenerative diseases [17]. In current study, we screened small molecules obtained from a natural compound library (The construction of designed library is described in the part of *Materials and Methods*) and identified a natural compound- luteolin, experimentally marked as D108, as a potential isoQC inhibitor. It can reduce pyroglutamate modification of CD47 and thus attenuate the interaction between CD47 and SIRPα in multiple myeloma H929 cells, which is mechanistically distinguished from current therapeutic strategy using CD47 antibody-based drugs that focus on CD47 blockade. Our study paves a way for *de novo* anti-tumor drug discovery that may avoid CD47 blockade-triggered side effects and arouse further robust interest for a better understanding of immune checkpoint signaling.

Materials and methods

Cell culture

Human multiple myeloma cell line NCI-H929 cells were kindly provided by Dr. Congying Wang (Shanghai Ten's People Hospital, China). Human colorectal cancer cell lines HCT116 and DLD1 cells were purchased from Shanghai Cell Bank, Chinese Academy of Sciences. HCT116 cells were cultured in DMEM supplemented with 10% fetal bovine serum (FBS, Gibco), 100 U/ mL penicillin, and 100 μg/ mL streptomycin (Invitrogen) at 37 °C in a humidified 5% CO_2 incubator, while DLD1 and H929 cells were cultured in RPMI 1640 supplemented with 10% fetal bovine serum, 100 U/ mL penicillin, and 100 μg/ mL streptomycin.

Natural compound library construction

Natural compounds used in the current study is kindly provided by our collaborator (Dr. Wang's lab). Briefly, raw plant drugs were ground and then soaked in 2.4 L of hydrophobic acid at a ratio of 1:8 (g/mL) at 80 °C with constant stirring for 1 hr. The filtrate was collected after vacuum concentration in a rotary evaporator. The crudes were obtained by reduced pressure distillation in the rotary evaporator. The crudes were separated by reversed-phase silica gel column chromatography with methanol-water gradient elution. The eluting components of each bed volume were collected and detected by thin-layer chromatography. The development agent was chloroform: ether: methanol (10: 10: 1). After the development, 2% bismuth potassium iodide was used to develop the color, which was reddish brown. The components were enriched and product was obtained after vacuum concentration in the rotary evaporator at 50 °C, followed by homogeneity assessment, determination of molecular weight, composition analysis, fourier transform-infrared (FT-IR) spectrophotometry analysis and NMR analysis. Obtained natural compounds were suspended in DMSO for following experiments.

Western blotting

Cells were lysed in lysis buffer (50 mM Tris-HCl, pH 7.4, 150 mM NaCl, 1 mM EDTA, 1% Tritonx-100, 5% Glycerol and a cocktail of proteinase inhibitors). After lysis for 15 min in 4 °C, the soluble fraction of the cell lysate was isolated via centrifugation at 13,800 g in a microcentrifuge for 15 min at 4 °C. After mixed with loading buffer, the proteins were processed at room temperature, resolved via SDS-PAGE gel electrophoreses, and analyzed via immunoblotting. The proteins were detected using the Odyssey system (LI-COR Biosciences).

RNA extraction and quantitative real-time polymerase chain reaction (qRT-PCR)

Total RNA was isolated from cells as treated above by using TRIzol (TAKARA) according to the manufacturer's instructions. After isolation, 1 μg of mRNA was used to be converted to cDNA using the Prime ScriptTM RT reagent kit (Cat# DRR037A, Takara,). These reactions were performed in CFX96 (Bio-Rad, United States) and run pre-programmed program. The cycle threshold (Ct) values were collected and normalized to the level of respective Actin. The primers were listed as follows:

Actin-F: ACACTGTGCCCATCTACGAG.
Actin-R: TCAACGTCACACTTCATGATG.
CD47-F: GTACAGCGATTGGATTAACCTCC.
CD47-R: ACCACAGCGAGGATATAGGCT.

isoQC protein purification

The DNA with sequence coding for the human glutaminyl-peptide cyclotransferase-like protein (nucleotide entry: NP_060129) was synthesized and then inserted into the pGEX-4T-2 vector. The vector was transformed into Escherichia coli BL21 (DE3) competent cells (CB105, Tiangen Biotech, Beijing). The bacteria were grown in Terrific Broth containing ampicillin (70 μg/ mL) at 37°C until the cell density reached an OD_{600} of 0.8–0.9. The cultures were induced with 1 mM isopropyl β-D-thiogalactopyranoside for 8- 10 h at 20 °C. The bacteria were collected and resuspended in 50 mL PBS, and 1% Triton X-100 (v/v), 1% β-mercaptoethanol (v/v), PMSF (final concentration 1 mM) were added into the mixed solution. The bacterial cells were then harvested by centrifugation (4700 g for 30 min at 4 °C) followed by ultrasonic breaking. The resulted solution was clarified by centrifugation at 13,800 g for 30 min. GST-beads was suspended to the supernatant and was gently shook for 1 hour to bind the protein. The resulted protein solution was centrifuged at 1500 g for 5 min and the supernatant was discarded. At least 10-fold the volume of PBS was added to the pellet to sufficiently suspend the beads in the solution. Then the solution was clarified by centrifugation at 1500 g for 5 min and the supernatant was discarded. The above steps were repeated twice. 1 mL GST elution buffer was added to the pellet and the solution was shaken gently for 30 min following by centrifugation at 1500 g for 5 min. The supernatant was collected and was eluted with GST elution buffer at least twice. The supernatant was loaded onto SDS-PAGE electrophoresis to detect protein purity. The protein was stored at −80 °C.

Isolation of bone marrow-derived macrophages

Six-week-old C57BL/6 wild-type mice were obtained from Shanghai Experimental Animal Center (Shanghai, China). To obtain bone marrow derived macrophage BMDM, femora and tibiae were flushed with ice-cold PBS, and erythrocytes were lysed with RBC lysis buffer. Then bone

marrow cells were cultured in DMEM medium with 10% FBS (Gibco) and 100 U/ mL penicillin, and 100 μg/ mL streptomycin (Invitrogen) in the presence of 50 ng/mL mouse M-CSF (Macrophage-Colony Stimulating Factor) (PeproTech) for 7 days.

Compound treatment

1-(1H-Benzimidazol-6-yl)−5-(4-propoxyphenyl) imidazolidine-2,4-dione (PQ529) was synthesized by WuXiAppTec. Cells were plated and treated with different concentrations of isoQC inhibitor (PQ529) or compounds for 48 h, then cells were harvested and CD47 was detected by FACS.

Flow cytometry assay

Binding to cell surface CD47 was assessed by staining cells with fluorochrome-labeled antibodies clone CC2C6 (BioLegend, Cat. # 323102) and B6H12 (Abcam, Cat# ab134485) to human CD47 at a dilution of 1:100 in PBS containing 0.5% (w/v) BSA (Sigma) and 0.2% (w/v) sodium azide (Sigma) (FACS buffer) for 30 min at 4 ˚C, while protected from light. SIRPα binding to CD47 was assessed by incubating cells with PE labeled recombinant human SIRPα/ CD172α Protein, Fc tag (Cat. # SIA-HP252, ACRO Biosystems) for 1 hour at 4 ˚C, while protected from light.

Phagocytosis Assay were conducted as previously described [13]. Briefly, macrophages were plated 1×10^5 cells per well in a 24-well plate in complete DMEM medium, supplemented with M-CSF overnight before the experiment. Cancer cells were stained with 2.5 μM CFSE at 37 ˚C for 10 min. Each phagocytosis reaction reported in this work was performed by co-culture of target cells and macrophages for 2 h at 37 ˚C. Macrophages were identified with APC-labeled anti-F4/80 (Cat. # 123116, Biolegend), and flow cytometry (BD FACS verse) was performed. Phagocytosis was calculated as the percentage of $CFSE^+F4/80^+$ cells (Q2) among $F4/80^+$ cells (Q1+Q2): phagocytosis (%) = [Q2 / (Q1+Q2)] x100%.

Synthesis and formation of biotin-luteolin

The synthesis of compound Biotin-luteolin is outlined in supplementary Fig. S1. First, commercially available luteolin was protected by diphenyl and the OH of tert-butyl (14-hydroxy-3,6,9,12-tetraoxatetradecyl) carbamate was converted to the OTs, respectively. The 2-(2,2-diphenylbenzo[*d*] [1,3] dioxol-5-yl)−5,7-dihydroxy-4H-chromen-4-one was further substituted to tert-butyl(14-((2-(2,2-diphenylbenzo[*d*] [1,3] dioxol-5-yl)−5-hydroxy-4- oxo- 4H-chromen-7-yl) oxy)- 3,6,9,12-tetraoxatetradecyl) carbamate in presence of 2,2- Dimethyl-4-oxo-3,8,11,14,17-pentaoxa-5-azanonadecan-19-yl-4-methylbenzenesulfonate. After removal of the tert-butylcarbonate (Boc) protecting group, the resulting primary amine intermediate reacted with a carboxylic acid to produce N-(14-((2-(2,2-diphenylbenzo[*d*]-[1,3]-dioxol-5-yl)−5-hydroxy-4-oxo −4H-chromen-7-yl)-oxy)−3,6,9,12-tetraoxatetradecyl)−5-((3a*S*,4*S*,6a*R*)−2-oxohexahydro-1H-thieno[3,4-*d*]-imidazol-4-yl)-pentanamide. This was deprotected of the diphenyl to afford final compound Biotin-luteolin.

GST pull-down assay

Biotin- or biotin-luteolin-conjugated agarose beads were prepared as described below. 15 μL of streptavidin agarose beads (50% slurry, pre-washed) and 10 μL of 10 mM Biotin- or biotin- luteolin were mixed in a 1.5 mL tube and incubated at room temperature for 30 min with occasional mixing. 1 μL BSA (10 mg/ mL) and 200 μL binding buffer were added to the mixture solution and incubated in cold room with rotation for 2 h. 8 μg of GST-isoQC protein were then added to the above solution and was incubated with rotation overnight at 4 ˚C. After incubation, the beads were washed 5 times with washing buffer (10 min each) in cold room. At last wash, buffer was removed as much as possible. Remaining material was loaded with 10∼15 μL of 2x SDS loading buffer and determined by Western blotting assay.

Molecular docking studies

All the procedure was performed using Maestro software (Schrodinger LLC). The crystal structure of human isoQC was taken from protein database bank (PDB ID: 3PB7). Then, the protein was processed using the 'Protein Preparation Wizard' workflow in Maestro to adding bond orders and hydrogens. All het atm residues and crystal water molecules beyond 5 Å from het group were removed. The co-crystallized molecule was removed from the system. Compound D108 was built by LigPrep module by OPLS-2005 force field. Glide module was used as docking program. The active site was defined using the zinc as the center. The docking box was placed on the centroid of the binding ligand in the optimized crystal structure as described above.

Isothermal titration calorimetry (ITC)

Isothermal titration calorimetry experiments were performed using a MicroCal iTC200 (GE Healthcare) at 25 ˚C. The isoQC protein was supplemented with buffer containing 10 mM HEPES, pH 7.5, 3.4 mM EDTA, 0.005% Tween-20, 150 mM NaCl, and 0.005% dimethyl sulfoxide (DMSO). Small molecules were diluted in the same buffer from 10 mM stock in DMSO. All solutions were degassed before titrations were performed. The sample cell was filled with 250 μL small molecule (0.2 μM) and the syringe was filled with 60 μL protein (9.57 μM). The titration consisted of an initial injection of 0.4 μL followed by 17 injections of 2 μL. To determine the baseline, the protein was titrated into the same buffer without the small molecules under the same conditions. Data was analyzed with the software Origin 7.0 (OriginLab) using the one set of sites model.

Statistical analysis

GraphPad Prism 8 software was used for data analysis. All experiments were repeated at least twice. Data were shown as mean ± SD. Statistical significance was evaluated by Student's *t*-test. P value was considered statistically significant. In the graphed data $*$, $**$ and $***$ denote *p*values of < 0.05, 0.01 and 0.001, respectively. In the figures, ns represents not significant data.

Results

isoQC is associated with decreased patient survival in multiple types of cancers

Our previous work reported that isoQC is significantly upregulated in multiple types of cancers [13]. To investigate whether high expression of isoQC is correlated with patient survival, we employed OncoLnc analysis that can extract patient survival data from publicly available The Cancer Genome Atlas (TCGA) datasets to generate Kaplan plot [18]. The expression data in OncoLnc for mRNAs analysis were transformed into normalized RSEM values via "rsem.genes.normalized_results". The median-expression values were calculated as 533.72, 269.34, 130.98, 211.35, 236.92, 347.39 for skin cutaneous melanoma, kidney renal papillary cell carcinoma, brain lower grade glioma, kidney renal clear cell carcinoma, sarcoma and rectum adenocarcinoma, respectively. Using median expression as the cut-off value to define high expression, we found that isoQC is strongly associated with a decreased overall survival rate of multiple types of cancers including skin cutaneous melanoma,

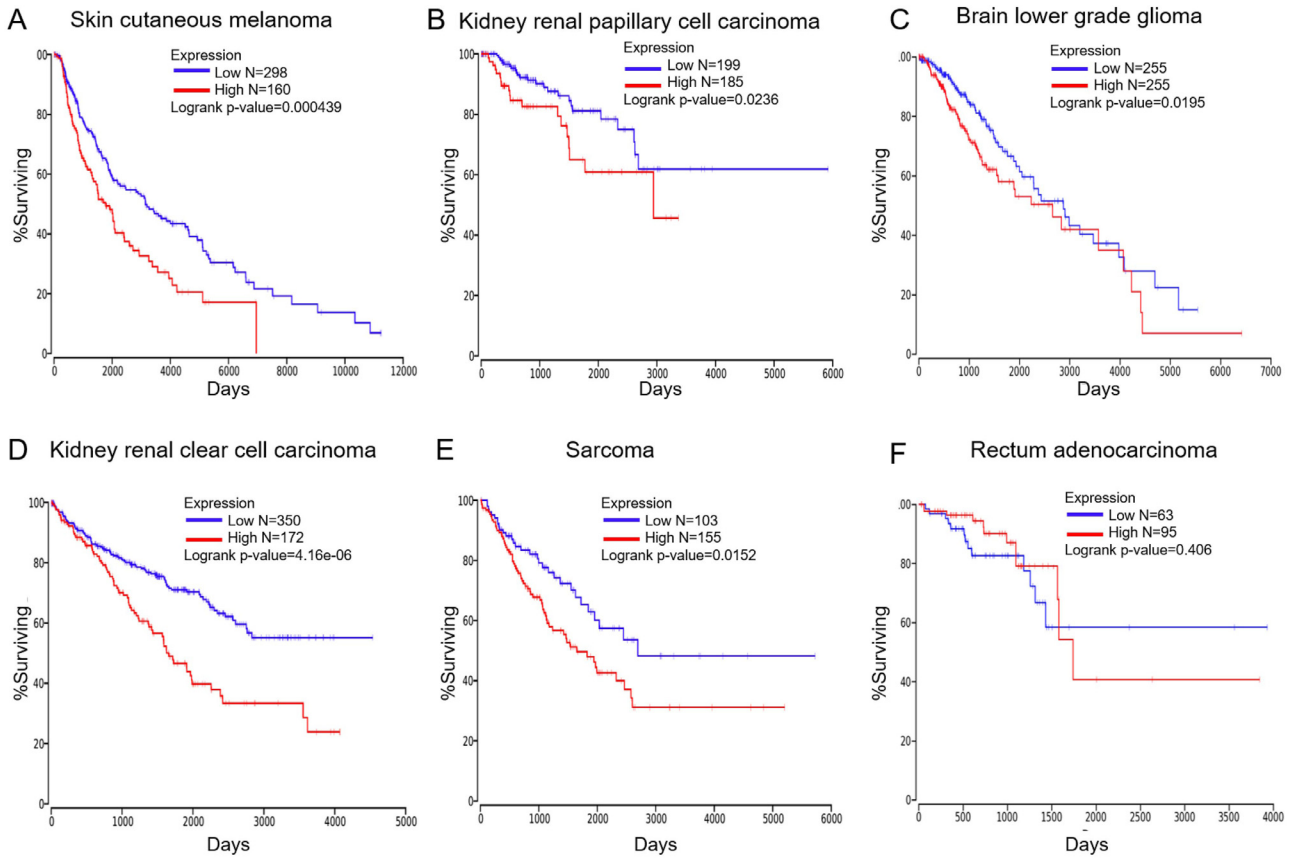

Fig. 1. *isoQC is negatively correlated with the survival rate of patient.* Correlation of isoQC expression with the prognosis in patients with multiple types of cancers, such as **(A)** Skin cutaneous melanoma**, (B)** Kidney renal papillary cell carcinoma**, (C)** Brain lower grade glioma**, (D)** Kidney renal clear cell carcinoma**, (E)** Sarcoma and **(F)** Rectum adenocarcinoma using OncoLnc. (The red: patients with high expression levels of isoQC; the blue: patients with low expression levels of isoQC).

kidney renal papillary cell carcinoma**,** brain lower grade glioma**,** kidney renal clear cell carcinoma**,** sarcoma and rectum adenocarcinoma (Fig. 1), suggesting that isoQC may act as a potential therapeutic target for anti-tumor immunity.

Screening natural compounds to identify potential inhibitors for pGlu modification of CD47

Both Logtenberg et al. [12] and our previous work [13] demonstrated that isoQC is an essential regulator that dictates the interaction between CD47 and SIRPα, which plays an important role in CD47-related immune checkpoint signaling. To identify potential small-molecules that affect isoQC activity, we established a biochemical screening system utilizing fluorescence-activated cell sorting assay (FACS), followed by the surface-expression analysis of CD47 using anti-human CD47 monoclonal antibody B6H12 (BD, Cat# 563760) and antibody CC2C6 (Biolegend, Cat# 323124) that has been confirmed to specifically recognize pGlu-modified CD47 at its N-terminus [13]. We used the isoQC inhibitor, PQ529, as a positive control [19] and screened 112 compounds in treatment of multiple myeloma H929 cells (Fig. 2A). We found that compound D48, D79, D108, D110 or D119 could down-regulate the pGlu modification of CD47 with relative inhibition around 21.1%, 20.2%, 35.2%, 18.4%, or 22.5%, respectively, while their total surface levels of CD47 remained unaffected (Fig. 2B, 2C **and supplementary Fig. S1 and Fig. S2**). To confirm such inhibition caused by these compound treatments is not a unique instance, we further detected the surface-expression of CD47 and its pGlu modification in DLD1 and HCT116 cells through which similar results were obtained (Fig. 2D–2G **and supplementary Fig. S1 and Fig. S2**). Particularly, luteolin (marked as D108) decreased the pGlu modification of CD47 with inhibitory efficiency of 35.2%, 20% and 17% in H929, DLD1 and HCT116 cells, respectively. Our data indicated that luteolin is a potential inhibitor for pGlu modification of CD47.

Luteolin directly interacts isoQC protein

To test whether luteolin binds to isoQC protein in vitro, we performed biotinylated protein interaction pull-down assay. Bio-luteolin was synthesized as shown in Fig. 3A**, supplementary Fig. S3 and Fig. S4**. Our data showed that bio-luteolin tightly bound to isoQC protein, which validates a direct interaction between luteolin and isoQC (Fig. 3B). To explore how luteolin interacts with isoQC protein, information regarding the possible binding mode of luteolin was obtained through an *in silico* docking analysis. We utilized the X-ray crystal structure of human isoQC complexed with a known inhibitor (PDB ID: 3PB7). Glide SP (Standard Precision) docking was carried out, showing that luteolin was docked very well at the active site of isoQC (Fig. 3C). The ortho-hydroxy groups in pyrocatechol part (Part I in Fig. 3D) was translocated into tunnel-shaped pocket and chelated with zinc atom deep in the pocket (Fig. 3C). Two hydroxy groups formed hydrogen-bonding interaction with amino acids Asp269 and Glu225, respectively (Fig. 3D). The phenyl group in pyrocatechol part (Part I) formed a $\pi-\pi$ stacking interaction with the side chain of Trp350 (Fig. 3D). The phenol group of the chromone core was pointed to solvent region and the 4H-chromen-4-one core (Part II) presented $\pi-\pi$ interaction with residue Trp231, which is located at the backside of the active-site opening (Fig. 3D). The carbonyl group of the chromone core formed hydrogen bonding interaction with the residue Glu325 (Fig. 3D). Together, these data demonstrated that luteolin directly interacts isoQC protein.

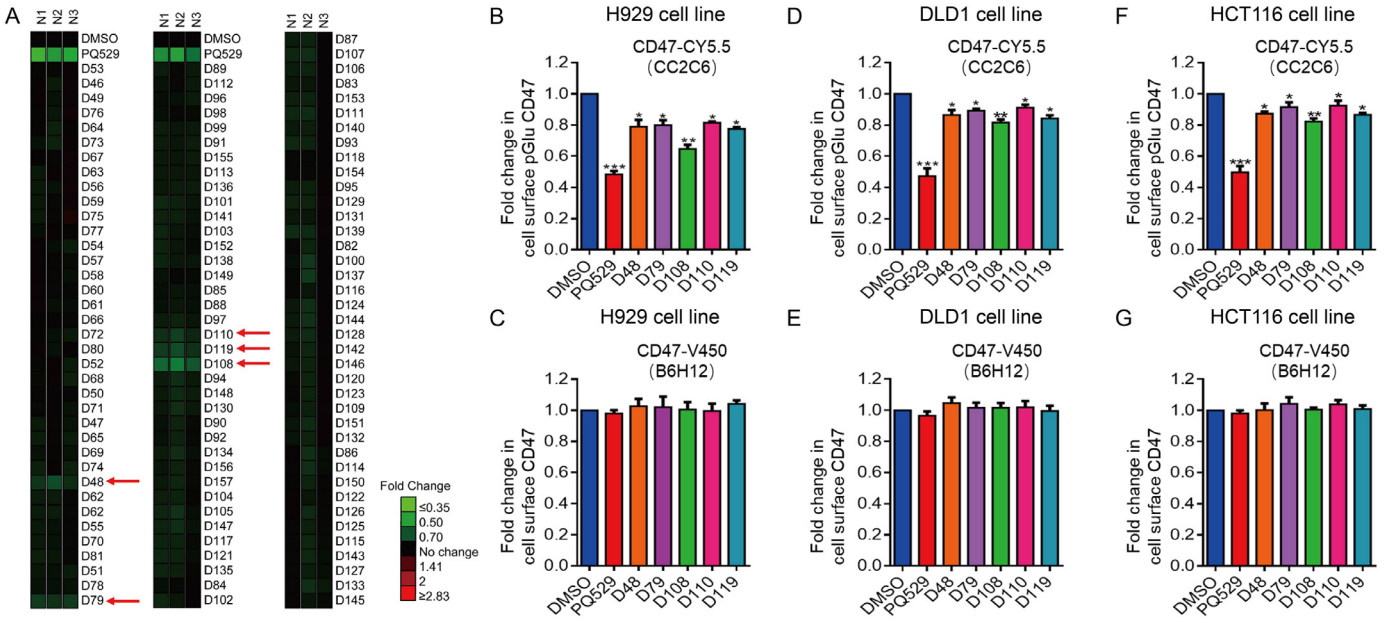

Fig. 2. Natural compounds screening.

A. Analysis of CD47 surface expression. H929 cells were treated with 10 μM isoQC inhibitor (PQ529) or other compounds as indicated for 48 h followed by FACS analysis using anti-CD47 CC2C6 monoclonal antibody. Their relative median fluorescence intensity (MFI) shown in the heatmap was displayed compared to those of DMSO treated samples (control). Error bars represent standard deviation from three independent experiments ($^{*}p < 0.05$, $^{**}p < 0.01$, $^{***}p < 0.001$).

B, D and F. FACS analysis of pGlu levels of CD47 using anti-CD47 CC2C6 monoclonal antibody in H929 cells, DLD1cells, HCT116 cells, respectively, after the treatments of 10 μM PQ529 or compounds D48, D79, D108, D110 and D119 for 48 h. Error bars represent standard deviation from three independent experiments ($^{*}p < 0.05$, $^{**}p < 0.01$, $^{***}p < 0.001$).

C, E and G. FACS analysis of cell surface levels of CD47 using anti-CD47 B6H12 monoclonal antibody in H929 cells, DLD1cells, HCT116 cells, respectively, after the treatments of 10 μM PQ529 or compounds D48, D79, D108, D110 and D119, respectively, for 48 h.

Luteolin is a novel inhibitor of isoQC

The chemical structure of luteolin, a 3,4,5,7-tetrahydroxy flavone, is shown in Fig. 4A. Since isoQC has been reported to control the interaction between CD47 and SIRPα [12], we further examined the binding affinity of luteolin to isoQC. To this end, we performed isothermal titration calorimetry (ITC) assay and the dissociation constant, K_D value, was calculated from experimentally determined values of Ka (K_D =1/Ka) using a single set of sites model analyzed by Origin 7.0 (OriginLab). We found that luteolin strongly bound to isoQC protein with a K_D value of 9.4 μM (Fig. 4B) which is slightly less than that of reported isoQC inhibitor PQ529 whose K_D value is around 1.7 μM [19] (Fig. 4C). The signature plots representing thermodynamics parameters of titration demonstrated that the enthalpy change $\Delta H = -320{,}000$ Kcal/ mol, entropy change $\Delta S = -1070$ Kcal/ mol, and the number of binding sites $N = 0.46$ (Fig. 4B). The inhibition of luteolin on proliferation activity was also investigated in H929 cells by counting cell number 4 days after the treatment of PQ529 or luteolin. Luteolin exhibited a remarkable inhibition on tumor cell proliferation, which has similar function of a known isoQC inhibitor, PQ529 (Fig. 4D). These results together indicated that luteolin is a novel inhibitor of isoQC activity.

Luteolin reduces pGlu modification of CD47 and its surface binding to SIRPα

Since isoQC is critical for pGlu formation of CD47 at the N-terminus, we next examined the effect of luteolin on the CD47 pGlu formation in H929 cells. Expression of CD47 and surface expression of pGlu CD47 in H929 cells were detected by anti-CD47 CC2C6 and B6H12 monoclonal antibodies, respectively, after 72-hr treatment with 10 μM luteolin. Our data showed that luteolin reduced pGlu formation of CD47 in a time-dependent way (Fig. 5A), while little effect on the surface-expression of CD47 was observed (Fig. 5B). Because pGlu formation usually protects proteins from proteasomal degradation, we also examined whether luteolin could affect the total protein expression of CD47. Endogenous transcriptional mRNA level of CD47 in H929 cells was examined by Quantitative Real-Time PCR assay and protein level of CD47 was demonstrated by western-blotting assay. Our data showed that luteolin had no significant inhibition on CD47 at both transcriptional and translational level (Fig. 5C and 5D). Since pGlu modification of CD47 has been demonstrated to block the interaction between CD47 and SIRPα [20], we therefore examined whether luteolin affected the binding of CD47 to SIRPα using a cell-based SIRPα binding assay. Our data showed that luteolin reduced the cell surface binding of CD47 to SIRPα similar as the known isoQC inhibitor-PQ529 (Fig. 5E and 5F), supporting our assumption that luteolin may function as a novel isoQC inhibitor.

Luteolin promotes macrophage-mediated phagocytosis

Blockade of CD47-SIRPα interaction has been shown to dramatically enhance tumor cell phagocytosis by macrophage in preclinical models of cancer [21,22]. To investigate whether luteolin can increase the macrophage-mediated phagocytosis of cancer cells, we performed in vitro phagocytotic assay by culturing H929 cells with mouse bone marrow-derived macrophages. Through employing this well-established phagocytosis assay, we showed that treatment of luteolin significantly enhanced the phagocytic capacity of macrophages targeting H929 cells (Fig. 6A and 6B) and DLD1 cells (Fig. 6C and 6D), indicating that luteolin may exert inhibitory effect on isoQC activity and thereby promote the macrophage phagocytosis of cancer cells via a repressed CD47-SIRPα signaling axis. Thus, we present the results of study as the schematic illustration concerning the different roles of luteolin, a new inhibitor targeting at pGlu modification of CD47, in macrophage-mediated phagocytosis of cancer cells and erythrocytes (Fig. 7), which may render a better visualization of how to fine-tune immune responses by using an organelle-specific enzyme.

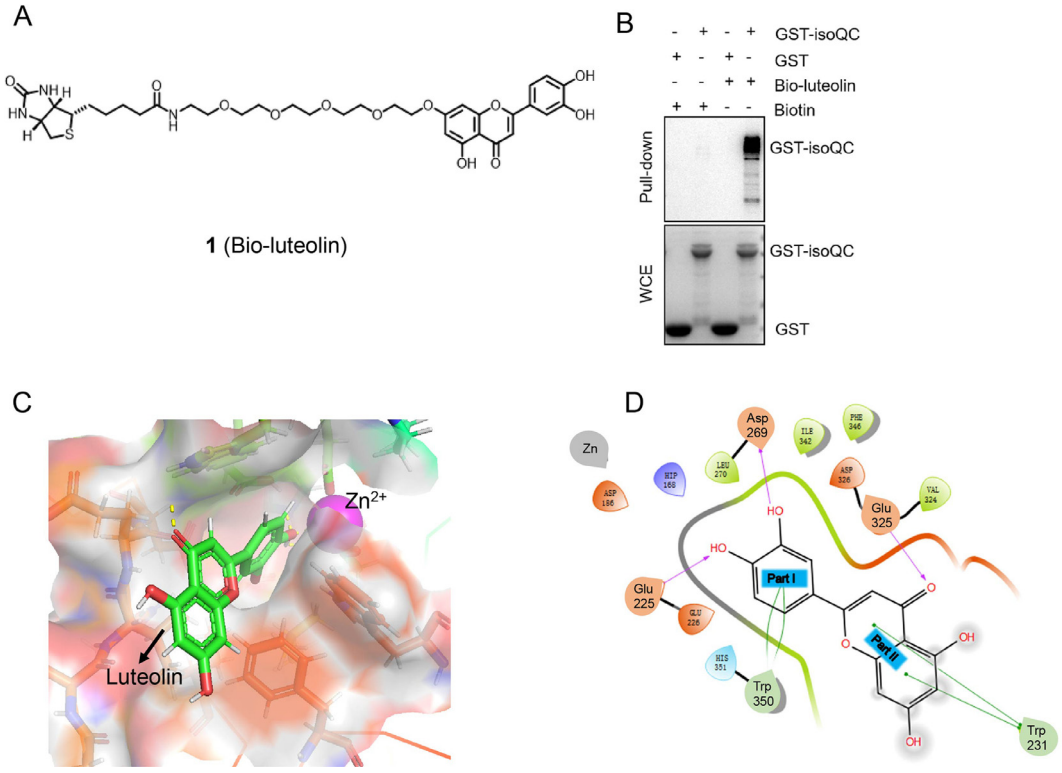

Fig. 3. Luteolin physically interacts with isoQC protein.
A. The chemical structure of biotin-luteolin (Bio-luteolin).
B. Luteolin binds to isoQC protein demonstrated by GST-pull down assay while whole cell protein extracts were used as an input control.
C. Computational molecular docking of luteolin to human isoQC. Luteolin was predicted to bind to the active site of isoQC. Luteolin is displayed as sticks with green carbon atoms, and zinc atom is shown as a purple ball.
D. Two-dimensional representation of the main interactions of luteolin with the active site residues of the isoQC. Hydrogen bonds are shown as purple arrows and the $\pi-\pi$ stacking interaction is marked as a green-arcs or arrows.

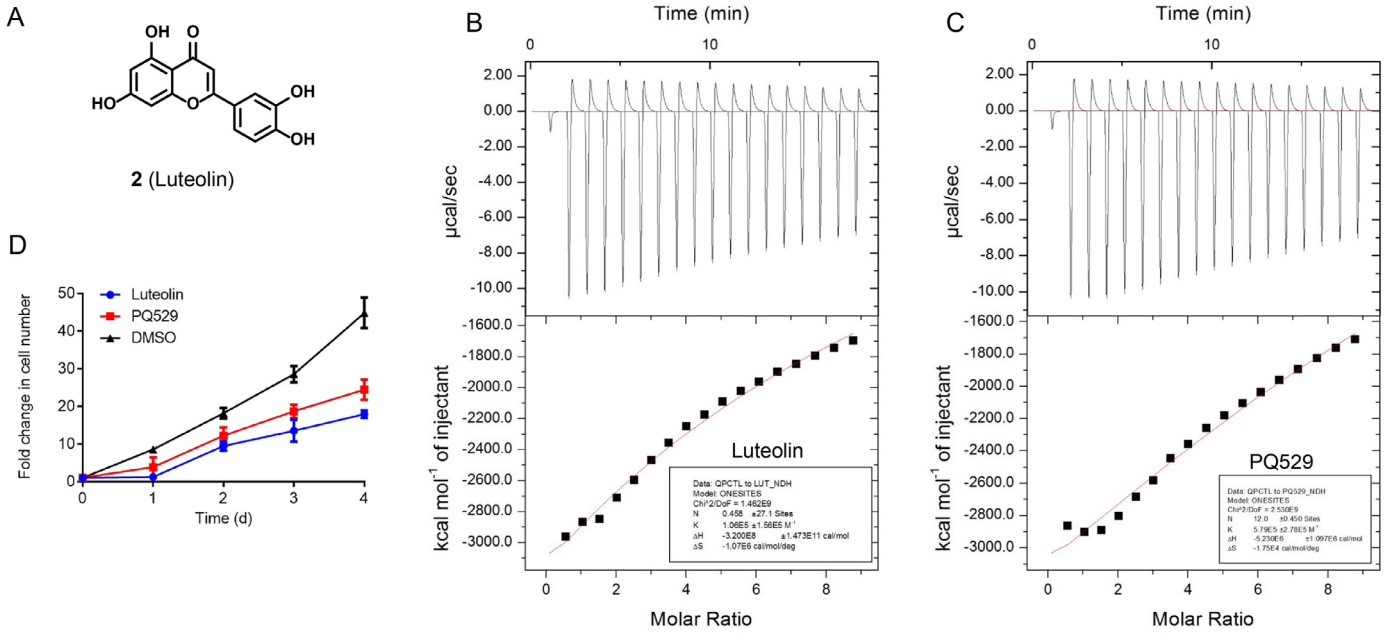

Fig. 4. Luteolin is a potent inhibitor of isoQC.
A. The chemical structure of luteolin.
B and C. Isothermal titration calorimetry (ITC) was employed to measure the binding affinities between isoQC protein and luteolin or PQ529.
D. Proliferation was assessed by counting cell numbers in triplicates for 4 days following treatment with PQ529 or luteolin. Error bars represent standard deviation from three independent experiments ($^{*}p < 0.05$, $^{**}p < 0.01$, $^{***}p < 0.001$).

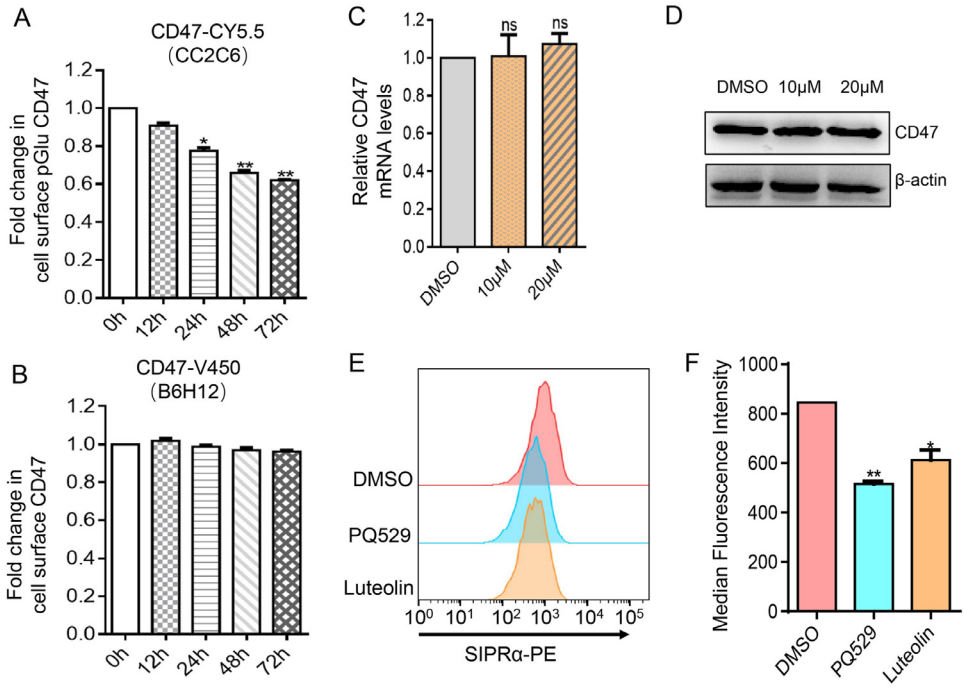

Fig. 5. Luteolin affects pGlu modification of CD47 and the cell surface binding of SIRPα.
A. Cell surface pGlu of CD47 using anti-CD47 CC2C6 monoclonal antibody in H929 cells following treatment with 10 μM luteolin for 72 h. The relative median fluorescence intensity (MFI) was displayed relative to DMSO control averages.
B.Cell surface expression of CD47 using anti-CD47 B6H12 monoclonal antibody in H929 cells following treatment with 10 μM luteolin for 72 h. The relative median fluorescence intensity (MFI) was displayed relative to DMSO control averages.
C. Endogenous transcriptional mRNA level of CD47 in H929 cells was demonstrated by Quantitative Real-Time PCR assay.
D Endogenous protein level of CD47 in H929 cells was demonstrated by western-blotting assay. The presented data is a representative image from three independent experiments with similar results.
E and F. FACS analysis of cell surface binding of SIRPα in H929 cells after treatment of PQ529 (10 μM) or luteolin (10 μM) for 48 h. The relative median fluorescence intensity (MFI) was calculated using DMSO sample as control. Error bars represent standard deviation from three independent experiments ($^{*}p < 0.05$, $^{**}p < 0.01$, $^{***}p < 0.001$).

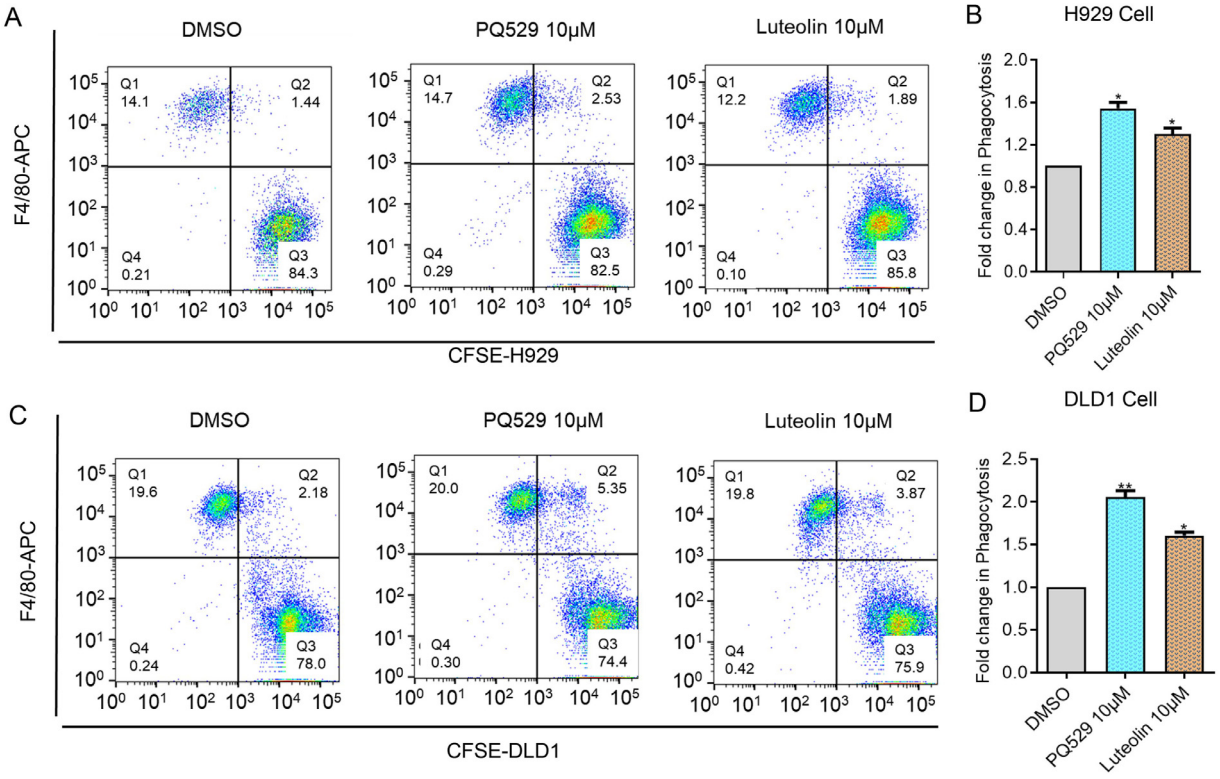

Fig. 6. Luteolin promotes macrophage-mediated phagocytosis.
A, B Phagocytosis of H929 cells by macrophages after treatment with PQ529 or luteolin (10 μM or 20 μM), which is normalized using DMSO treated sample as control. Phagocytosis was determined by the number of the CFSE^{+} labelled F4/80^{+} macrophages vs the total macrophages. The presented data is a representative image from three independent experiments with similar results, showing that there is a statistically significance between luteolin treated samples and those only with DMSO treatment ($^{*}p < 0.05$, $^{**}p < 0.01$, $^{***}p < 0.001$).
C, D Phagocytosis of DLD1 cells by macrophages after treatment with PQ529 or luteolin (10 μM or 20 μM), which is normalized using DMSO treated sample as control. Phagocytosis was determined by the number of the CFSE^{+} labelled F4/80^{+} macrophages vs the total macrophages. The presented data is a representative image from three independent experiments with similar results, showing that there is a statistically significance between luteolin treated samples and those only with DMSO treatment ($^{*}p < 0.05$, $^{**}p < 0.01$, $^{***}p < 0.001$).

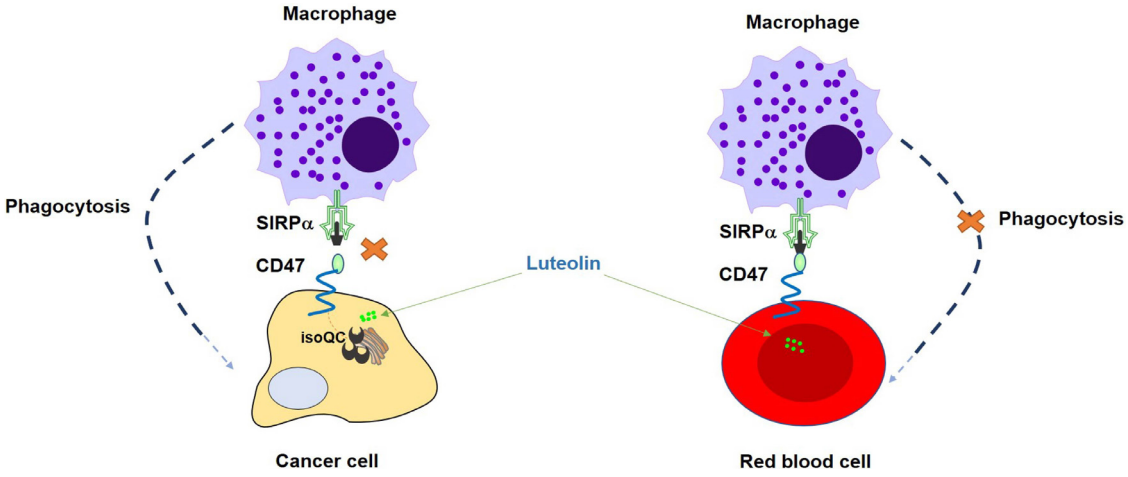

Fig. 7. Schematic model of how luteolin promotes macrophage-mediated phagocytosis of cancer cells.

Discussion

Cancer is well-established as a heterogeneous entity in terms of clinical presentation, genetic findings, proteomic architecture and metabolic profiles [23]. Due to the heterogeneity, tumor cells employ different mechanisms to resist the targeting agent [24]. Thus, inevitable drug resistance becomes the biggest hurdle to targeted cancer therapy with an unfortunate fact that conventional cytotoxic approaches exhibit limited effectiveness [25], resulting in a constant search for therapeutics with improved outcome, such as immunotherapy that utilizes and enhances the normal capacity of the patient's immune system [25]. For example, the renal cell carcinoma (RCC) represents a heterogeneous group of kidney neoplastic diseases, among which the kidney renal clear cell carcinoma was one of the highest incidence subtypes with poor prognosis [26]. Emerging evidence demonstrate that immunotherapy is the best treatment option for patients with metastatic or advanced RCC, supported by the clinical outcomes showing that combination immunotherapy based on a variety of principles has promising prospects [27]. Also, sarcomas are very heterogeneous characterized by an extensive group of divergent malignant diseases only sharing a common tag of being derived from mesenchymal cells [28]. Therefore, preventing tumors with huge heterogeneity (i.e. RCC and sarcoma) from immune escape is particularly important for the successful clinical implementation targeting these diseases with huge heterogeneity.

Recently, immune checkpoint blockade therapy has become a powerful weapon against the tumor immune escape. Accumulating evidence demonstrate that antibody drugs have obvious advantages, such as being of broad applicability across cancer types and durable clinical response due to immune memory [3]. Therefore, a range of immune checkpoint blockade therapeutic strategies targeting at different ligand-immunoreceptor engagement have attracted extensive attention in the fields of both cancer biology and pharmacological research, which have been demonstrated experimentally and translated into clinical treatments of various cancer types. Among these strategies, CD47-SIRPα blockade therapy is a hot-spot of research.

It has been reported that CD47 expression level was markedly elevated in high-risk patients with RCC, leading to a robust interest in targeting CD47 of RCC patients [29]. Simultaneously, early trials for immune checkpoint inhibitors in sarcomas have been carried out, indicating that CD47 inhibitors may be particularly worthwhile to pursue in treatment of sarcoma patients across various subtypes [30]. Yet, effective interception of CD47-SIRPα signaling axis has remained stubbornly elusive for new drug target discovery since current therapeutic strategies using CD47 antibody-based drugs, although initially inspiring, are deficient in their ability to evade erythrocyte destruction accompanied with CD47 blockade [4,7]. To address this issue, our lab made great efforts in identifying novel regulators and reported that inhibition of isoQC, a Golgi-resident enzyme lacking in mature erythrocyte, satisfied the requirements for disrupting the CD47-SIRPα interaction specifically on the surface of cancer cells by reducing the levels of pGlu-containing CD47 and its consequent binding affinity to SIRPα [13], a similar conclusion to the research article from Dr. Schumacher's lab [12].

To bridge the gap from our proposed theory to its clinical translation using pGlu modification of human CD47 N-terminal peptide as a therapeutic target, we confirmed there exists a negative correlation between isoQC expression and the prognosis in patients with multiple types of cancers particularly including RCC and Sarcoma (Fig. 1), leading to a natural compound screening for novel isoQC inhibitors in current research (Fig. 2) through which luteolin was brought into our interest because of its direct interaction with isoQC (Fig. 3) and capability of suppressing isoQC activity (Fig. 4). Therefore, luteolin exerted inhibitory effect on pGlu modification of CD47, a proved biomarker that can faithfully predict the CD47-SIRPα interaction [13], in a time-dependent manner (Fig. 5A). Most importantly, luteolin treatment in cancer cells exhibits a remarkable repression on the binding affinity of CD47 to SIRPα (Fig. 5) and consequently upregulates macrophage-mediated phagocytosis of cancer cells (Fig. 6). In parallel, our results also showed that treatment with luteolin had nothing to do with erythrocyte destruction (**Supplementary Fig. S5**) since there was no sign of erythrocyte elimination when erythrocytes and macrophages were co-cultured together (**Supplementary Fig. S6**). We also noticed that PQ529, a known isoQC inhibitor, was only effective for treatment of glomerulonephritis in chronic kidney disease when rats were orally administered with PQ529 (30 and 100 mg/kg) twice a day for 3 weeks. The data collected from in vivo studies indicated that PQ529 may have poor oral bioavailability, highlighting a plausible reason why clinical translations of isoQC inhibitors are currently limited [19]. To avoid the same thing happen to luteolin, we will use luteolin as a lead compound for structure optimization and investigation of the structure-activity relationship for isoQC in the future, which may greatly benefit the discovery of more potent isoQC inhibitors for cancer immunology therapy.

Our study highlights a new strategy with potential for clinical application which overcomes the disadvantages associated with current CD47 blockade-based drugs, and opens a door for treatment of refractory solid tumors tagged with remarkable heterogeneity in tissue components and function. Conclusively, we not only offer a new lead compound of isoQC inhibitor, Luteolin, for immunotherapeutic drug development but also shed light on the concept that posttranslational modification may serve practically as the therapeutic target of an anti-tumor immune response by counteracting the suppressive function of some immune checkpoint,

which is previously focused on absolute interruption of adaptor-protein association. Thus, our study breaks a new avenue for mediation of immune checkpoint signaling according to the specific distribution of a posttranslational-modifying enzyme.

Author contributions

Conceptualization, L.Y., P.W. and X.G.; Methodology, Z.L. and D.R.; Validation, M.L., J.W., X.C., W.T.; Formal Analysis, Z.L., D.R. and L.Y.; Investigation, Z.L. and D.R.; Resources, H.W., X.C., S.X. and X.G.; Data Curation, Z.L., D.R. and L.Y.; Writing-Original Draft Preparation, Z.L. and L.Y.; Writing-Review & Editing, X.G.; Visualization, Z.L., D.R. and L.Y.; Supervision, P.W.; Project Administration, P.W.; Funding Acquisition, W.T., S.X., P.W. and X.G. All authors have read and agreed to the published version of the manuscript.

Funding

This work is supported by the National Natural Science Foundation of China (Grant numbers 81625019, 31870900, 82073086, 81874198), Natural Science Foundation of Shanghai (20ZR1468400) and Young Elite Scientists Sponsorship Program by CAST (2019-2021QNRC001).

Declaration of Competing Interest

All authors declare no conflict of interest.

Acknowledgments

We would like to thank Prof. Hongbing Wang from Tongji University for kindly providing the compounds for screening, Prof. Jumei Shi and Yingcong Wang from Shanghai Tenth's People Hospital for providing the NCI-H929 cell line. We thank the staff members of the Large-scale Protein Preparation System at the National Facility for Protein Science in Shanghai (NFPS), Zhangjiang Lab, China for providing technical support and assistance in data collection and analysis. We also thank Dr. Xinbo Wang and Dr. Zan Li for critically reading the manuscript. We also thank the members of the Wang lab for their assistance.

Supplementary materials

Supplementary material associated with this article can be found, in the online version, at doi:10.1016/j.tranon.2021.101129.

References

[1] S. Kruger, M. Ilmer, S. Kobold, B.L. Cadilha, S. Endres, S. Ormanns, G. Schuebbe, B.W Renz, J.G. D'Haese, H. Schloesser, et al., Advances in cancer immunotherapy 2019 - latest trends, J. Exp. Clin. Cancer Res. 38 (2019) 268, doi:10.1186/s13046-019-1266-0.
[2] A. Ribas, J.D. Wolchok, Cancer immunotherapy using checkpoint blockade, Science 359 (2018) 1350–1355.
[3] X. He, C. Xu, Immune checkpoint signaling and cancer immunotherapy, Cell Res. 30 (2020), doi:10.1038/s41422-020-0343-4.
[4] W. Zhang, Q. Huang, W. Xiao, Y. Zhao, J. Pi, H. Xu, H. Zhao, J. Xu, C.E. Evans, H. Jin, Advances in anti-tumor treatments targeting the CD47/SIRPalpha axis, Front. Immunol. 11 (2020) 18, doi:10.3389/fimmu.2020.00018.
[5] R. Advani, I. Flinn, L. Popplewell, A. Forero, N.L. Bartlett, N. Ghosh, J. Kline, M. Roschewski, A. LaCasce, G.P. Collins, et al., CD47 blockade by Hu5F9-G4 and rituximab in non-Hodgkin's lymphoma, N. Engl. J. Med. 379 (2018) 1711–1721, doi:10.1056/NEJMoa1807315.
[6] A.R. Jalil, J.C. Andrechak, D.E. Discher, Macrophage checkpoint blockade: results from initial clinical trials, binding analyses, and CD47-SIRPalpha structure-function, Antib Ther 3 (2020) 80–94, doi:10.1093/abt/tbaa006.
[7] V. Buatois, Z. Johnson, S. Salgado-Pires, A. Papaioannou, E. Hatterer, X. Chauchet, F. Richard, L. Barba, B. Daubeuf, L. Cons, et al., Preclinical development of a bispecific antibody that safely and effectively targets CD19 and CD47 for the treatment of B-Cell lymphoma and leukemia, Mol. Cancer Ther. 17 (2018) 1739–1751, doi:10.1158/1535-7163.
[8] R. Ch, G. Rey, S. Ray, P.K. Jha, P.C. Driscoll, M.S.D. Santos, D.M. Malik, R. Lach, A.M. Weljie, J.I. MacRae, et al., Rhythmic glucose metabolism regulates the redox circadian clockwork in human red blood cells, Nat. Commun. 12 (2021) 377, doi:10.1038/s41467-020-20479-4.
[9] J. Sharon, B.O.P. Wiback 1, Extreme pathway analysis of human red blood cell metabolism, Biophys. J. 83 (2002) 808–818, doi:10.1016/S0006-3495(02)75210-7.
[10] H. Cynis, J.-.U. Rahfeld, A. Stephan, A. Kehlen, B. Koch, M. Wermann, H.-.U. Demuth, S. Schilling, Isolation of an isoenzyme of human glutaminyl cyclase: retention in the Golgi complex suggests involvement in the protein maturation machinery, J. Mol. Biol. 379 (2008) 966–980, doi:10.1016/j.jmb.2008.03.078.
[11] K.-.F. Huang, S.-.S. Liaw, W.-.L. Huang, C.-.Y. Chia, Y.-.C. Lo, Y.-.L. Chen, A.H.-J. Wang, Structures of human Golgi-resident glutaminyl cyclase and its complexes with inhibitors reveal a large loop movement upon inhibitor binding, J. Biol. Chem. 286 (2011) 12439–12449, doi:10.1074/jbc.M110.208595.
[12] M.E.W. Logtenberg, J.H.M. Jansen, M. Raaben, M. Toebes, K. Franke, A.M. Brandsma, H.L. Matlung, A. Fauster, R. Gomez-Eerland, N.A.M. Bakker, et al., Glutaminyl cyclase is an enzymatic modifier of the CD47- SIRPalpha axis and a target for cancer immunotherapy, Nat. Med. 25 (2019) 612–619, doi:10.1038/s41591-019-0356-z.
[13] Z. Wu, L. Weng, T. Zhang, H. Tian, L. Fang, H. Teng, W. Zhang, J. Gao, Y. Hao, Y. Li, et al., Identification of Glutaminyl Cyclase isoenzyme isoQC as a regulator of SIRPalpha-CD47 axis, Cell Res. 29 (2019) 502–505, doi:10.1038/s41422-019-0177-0.
[14] J. Zheng, M. Wu, H. Wang, S. Li, X. Wang, Y. Li, D. Wang, S. Li, Network pharmacology to unveil the biological basis of health-strengthening herbal medicine in cancer treatment, Cancers 10 (2018), doi:10.3390/cancers10110461.
[15] A. Gomathi, K.M. Gothandam, Investigation of anti-inflammatory and toxicity effects of mangrove-derived Streptomyces rochei strain VITGAP173, J. Cell. Biochem. 120 (2019) 17080–17097, doi:10.1002/jcb.28969.
[16] G. Sanchez, O. Estrada, G. Acha, A. Cardozo, F. Pena, M.C. Ruiz, F. Michelangeli, C. Alvarado-Castillo, The norpurpureine alkaloid from Annona purpurea inhibits human platelet activation in vitro, Cell Mol. Biol. Lett. 23 (2018) 15, doi:10.1186/s11658-018-0082-4.
[17] M. Sharifi-Rad, C. Lankatillake, D.A. Dias, A.O. Docea, M.F. Mahomoodally, D. Lobine, P.L. Chazot, B. Kurt, T.B. Tumer, A.C. Moreira, et al., Impact of natural compounds on neurodegenerative disorders: from preclinical to pharmacotherapeutics, J Clin Med. 9 (2020) 1061, doi:10.3390/jcm9041061.
[18] A Jordan, OncoLnc: linking TCGA survival data to mRNAs, miRNAs, and lncRNAs, PeerJ Comput. Sci. 2 (2016), doi:10.7717/peerj-cs.7767.
[19] N. Kanemitsu, F. Kiyonaga, K. Mizukami, K. Maeno, T. Nishikubo, H. Yoshida, H. Ito, Chronic treatment with the (iso-)glutaminyl cyclase inhibitor PQ529 is a novel and effective approach for glomerulonephritis in chronic kidney disease, Naunyn Schmiedebergs Arch. Pharmacol. (2020) *Online ahead of print*, doi:10.1007/s00210-020-02013-x.
[20] D. Hatherley, S.C. Graham, J. Turner, K. Harlos, D.I. Stuart, A.N. Barclay, Paired receptor specificity explained by structures of signal regulatory proteins alone and complexed with CD47, Mol. Cell 31 (2008) 266–277, doi:10.1016/j.molcel.2008.05.026.
[21] K. Weiskopf, N.S. Jahchan, P.J. Schnorr, S. Cristea, A.M. Ring, R.L. Maute, A.K. Volkmer, J.-.P. Volkmer, J. Liu, J.S. Lim, et al., Cd47-blocking immunotherapies stimulate macrophage-mediated destruction of small-cell lung cancer, J. Clin. Invest. 126 (2016) 2610–2620, doi:10.1172/JCI81603.
[22] D. Hazama, Y. Yin, Y. Murata, M. Matsuda, T. Okamoto, D. Tanaka, N. Terasaka, J. Zhao, M. Sakamoto, Y. Kakuchi, et al., Macrocyclic peptide-mediated blockade of the CD47-SIRPalpha interaction as a potential cancer immunotherapy, Cell Chem. Biol. 27 (2020) 1181–1191 e1187, doi:10.1016/j.chembiol.2020.06.008.
[23] S. Li, K.H. Young, L.J. Medeiros, Diffuse large B-cell lymphoma, Pathology 50 (2018) 74–87, doi:10.1016/j.pathol.2017.09.006.
[24] Z.-.F. Lim, P.C. Ma, Emerging insights of tumor heterogeneity and drug resistance mechanisms in lung cancer targeted therapy, J. Hematol. Oncol. 12 (2019) 134, doi:10.1186/s13045-019-0818-2.
[25] A.N. Miliotou, L.C. Papadopoulou, CAR T-cell therapy: a new era in cancer immunotherapy, Curr. Pharm. Biotechnol. 19 (2018) 5–18, doi:10.2174/1389201019666180418095526.
[26] C.L. Chaffer, R.A. Weinberg, A perspective on cancer cell metastasis, Science 331 (2011) 1559–1564, doi:10.1126/science.1203543.
[27] Y. Jian, K. Yang, X. Sun, J. Zhao, K. Huang, A. Aldanakh, Z. Xu, H. Wu, Q. Xu, L. Zhang, et al., Current advance of immune evasion mechanisms and emerging immunotherapies in renal cell carcinoma, Front. Immunol. 12 (2021) 639636, doi:10.3389/fimmu.2021.639636.
[28] J. Hatina, M. Kripnerova, K. Houfkova, M. Pesta, J. Kuncova, J. Sana, O. Slaby, R. Rodríguez, Sarcoma stem cell heterogeneity, Adv. Exp. Med. Biol. 1123 (2019) 95–118, doi:10.1007/978-3-030-11096-3_7.
[29] J.C. Xiaoliang Hua, Yang Su, Chaozhao Liang, Identification of an immune-related risk signature for predicting prognosis in clear cell renal cell carcinoma, Aging 12 (2020) 2302–2332.
[30] A.R. Dancsok, D. Gao, A.F. Lee, S.E. Steigen, J.-.Y. Blay, D.M. Thomas, R.G. Maki, T.O. Nielsen, 6, E.G.D., Tumor-associated macrophages and macrophage-related immune checkpoint expression in sarcomas, Oncoimmunology 9 (2020) 1747340, doi:10.1080/2162402X.2020.1747340.